JACS
JOURNAL OF THE AMERICAN CHEMICAL SOCIETY

Communication

pubs.acs.org/JACS

Membraneless, Room-Temperature, Direct Borohydride/Cerium Fuel Cell with Power Density of Over 0.25 W/cm^2

Nicolas Da Mota,[†,§] David A. Finkelstein,[†,§] Joseph D. Kirtland,[‡,§] Claudia A. Rodriguez,[†] Abraham D. Stroock,[‡] and Héctor D. Abruña*[,†]

[†]Department of Chemistry and Chemical Biology, Baker Laboratory, and [‡]Department of Chemical and Biomolecular Engineering, Olin Hall, Cornell University, Ithaca, New York 14853, United States

Supporting Information

ABSTRACT: The widespread adoption and deployment of fuel cells as an alternative energy technology have been hampered by a number of formidable technical challenges, including the cost and long-term stability of electrocatalyst and membrane materials. We present a microfluidic fuel cell that overcomes many of these obstacles while achieving power densities in excess of 250 mW/cm^2. The poisoning and sluggish reaction rate associated with CO-contaminated H_2 and methanol, respectively, are averted by employing the promising, high-energy density fuel borohydride. The high-overpotential reaction of oxygen gas at the cathode is supplanted by the high-voltage reduction of cerium ammonium nitrate. Expensive, ineffective membrane materials are replaced with laminar flow and a nonselective, porous convection barrier to separate the fuel and oxidant streams. The result is a Nafion-free, room-temperature fuel cell that has the highest power density per unit mass of Pt catalyst employed for a non-H_2 fuel cell, and exceeds the power density of a typical H_2 fuel cell by 50%.

The practical implementation of fuel cells presents numerous challenges. The use of hydrogen (H_2) is hindered by low volumetric energy density and storage difficulties. The H_2 must also be purified to contain less than 10 ppm CO to avoid poisoning the Pt anode;[1] the presence of CO arises from the production of H_2 from natural gas.[2] The use of methanol (MeOH), a more dense fuel by volume, suffers from poisoning and poor kinetics at the anode, as well as membrane crossover and poisoning at the cathode.[1,3−5] Despite these complications with fuels, the power output of the majority of fuel cells is oxidant-limited, relying on the high-overpotential reduction of O_2 at Pt and its alloys.[1] The overwhelming majority of low-temperature fuel cells rely on a proton exchange membrane (PEM), and in practice, this material is almost exclusively Nafion,[4−6] a high-cost material that causes the membrane to be one of the most expensive components of the fuel cell.[7]

Here we present a fuel cell that addresses many of these limitations, resulting in an unprecedented power density for a non-H_2, room-temperature fuel cell. A non-PEM, microfluidic fuel cell described previously[8,9] was used as a platform for evaluating the high-voltage redox pair, borohydride (BH_4^-)/cerium ammonium nitrate (CAN), along with a transport-enhancing, chaotic-mixing flow design.[10] Rather than a proton-selective membrane, the fuel cell uses a nonspecific convection barrier (polycarbonate filter paper, 0.2 μm pores, 10 μm thick, ∼10% open area) to separate fuel and oxidant streams. The barrier allows diffusive transport through the pores while precluding convective mixing of the fuel and oxidant streams. With a small ratio of pore diameter to channel cross-sectional dimensions, the barrier serves as a smooth, no-slip boundary for the flow. Though uniaxial laminar flow along the streamwise direction aids in the separation of fuel and oxidant, it also results in limited transport to the anode and cathode. Grooved electrodes (which give rise to transport-enhancing, chaotically stirred flow) were employed to create separate mixing regions in the two streams, effecting much higher current and power densities and enhancing fuel utilization.[10] The fuel and oxidant both exhibited rapid kinetics at Pt and high solubilities, allowing the fuel cell to be run at room temperature and higher current densities, respectively.[11,12] While most room-temperature MeOH,[4] BH_4^-,[5] and microfluidic[13] fuel cells have power densities on the order of 50 mW/cm^2 or less, our fuel cell generated 270 mW/cm^2, with 400 mA/cm^2 delivered at 0.65 V (Figure 1).

Comparisons between our system and other high-power fuel cells are difficult, largely because our electrodes are essentially flat (total area = geometric area), whereas in most reports, porous carbon supports with nanoparticulate catalysts are used to boost the microscopic electrode area to many times the geometric area. Power densities are then determined using only the geometric area. Comparing power generated per catalyst mass loading provides a very different assessment, especially since our vapor-deposited, 95 nm thick Pt electrodes hold just 0.2 mg Pt/cm^2, on the order of an H_2 fuel cell,[14] while high-performing MeOH and BH_4^- fuel cells typically use 2−8 and 1−2 mg of Pt/cm^2, respectively. Normalizing power to catalyst mass also provides a better systems-level assessment, since Pt serves as a primary cost driver for fuel cells.[7] The best MeOH fuel cells generate 2−30 mW/mg Pt, BH_4^- fuel cells 10−220 mW/mg catalyst (Pt, Pd, Ni, or Au), typical H_2 fuel cells ∼800 mW/mg Pt,[15] and our fuel cell 1230 mW/mg Pt. Additionally, MeOH and BH_4^- are typically employed at concentrations of 1.5−3 M, which are 10−20 times our 0.15 M BH_4^-, and operating temperatures for the BH_4^- fuel cells are often 60 °C or higher.[4,5] Several vanadium-based microfluidic fuel cells with

Received: December 16, 2011
Published: March 28, 2012

dx.doi.org/10.1021/ja211751k | J. Am. Chem. Soc. 2012, 134, 6076−6079

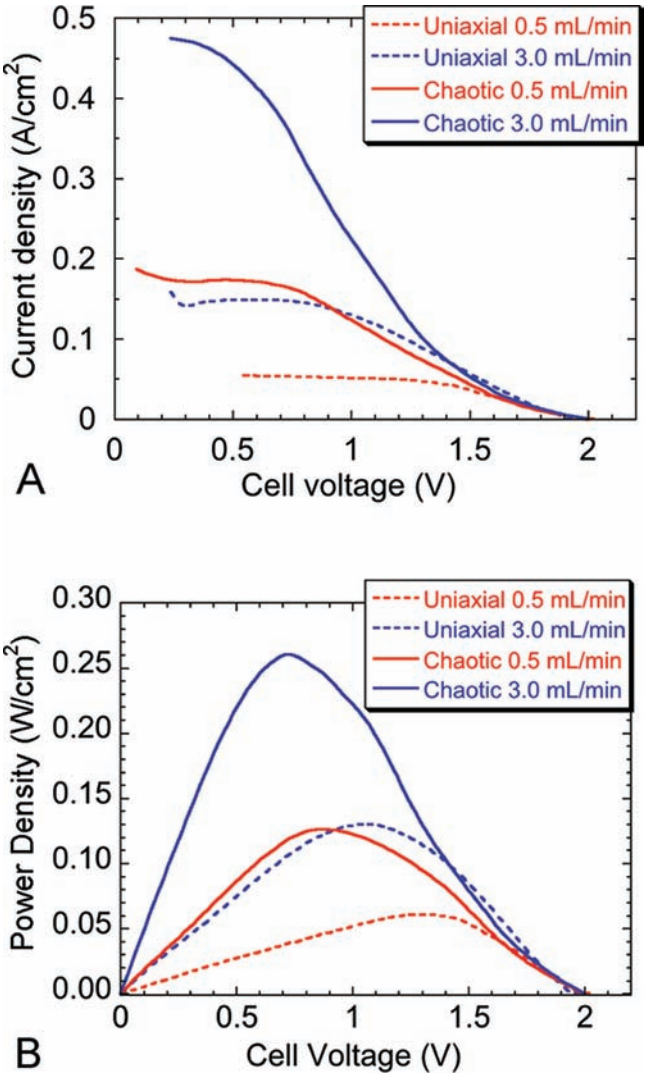

Figure 1. (A) Load curves and (B) power curves for fuel cell operation with 0.15 M $NaBH_4$ in 3 M NaOH and 0.5 M CAN in 1 M HNO_3. Dotted lines show operation with uniaxial flow. Solid lines show operation with chaotic flow, which enhances transport of fuel and oxidant to the electrodes.

Table 1. Reactions of the Fuel and Oxidant

reaction	E^0 (V vs NHE)	E_{onset} at Pt (V vs NHE)
$BH_4^- + OH^- \rightleftarrows H_2BO_3^- + 5H_2O + 8e^-$	−1.24[a]	−0.8[a]
$Ce^{4+} + e^- \rightleftarrows Ce^{3+}$	+1.72	+1.5[b]

[a]In 1 M NaOH. [b]In 1 M HNO_3.

similar current and power densities also use porous electrodes and 2 M fuel, though they enjoy the advantage of employing non-Pt carbon catalysts.[16,17] Only non-commercial, specialty H_2 fuel cells exceed the power per catalyst loading presented here.[15]

Direct BH_4^- fuel cells are of great current interest due to the theoretical yield of $8e^-$/molecule of BH_4^- at −1.2 V vs NHE and the lack of anode poisoning from CO impurities, but many investigators use Au rather than Pt anodes, resulting in significant system power loss,[11] and none have used CAN as an oxidant[5] ($1e^-$ at +1.7 V vs NHE). Table 1 summarizes the fuel cell reactions, their standard reduction potentials (E^0) in

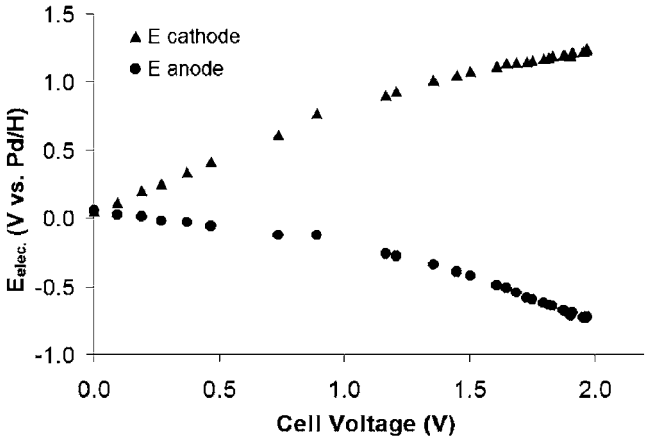

Figure 2. Plot of anode and cathode potentials vs cell voltage during operation of the BH_4^-/CAN microfluidic fuel cell. Between a cell voltage of 2.0 and 1.0 V, the anode potential changes more dramatically than the cathode potential (sacrificing more potential to drive the corresponding electrode reaction), indicating that BH_4^- is more limiting than CAN in the high-power region of fuel cell operation.

base and acid, and our observed potentials for the onset of significant current from the reaction (E_{onset}). Voltage was maximized using a dual-electrolyte configuration, in which base lowers the potential of the fuel and acid raises that of the oxidant.[7] Acid and base are consumed in the electrochemical reactions, directly converting the free energy of their association reaction ($H^+ + OH^- \rightleftarrows H_2O$) into voltage (for equimolar acid and base, $\Delta G = -FV_{\Delta pH} = -RT \ln K_w^{-1}$, with $V_{\Delta pH} = 0.828$ V for 1 M acid and 1 M base[18,19]). The BH_4^-/CAN pair is uniquely suited to such a system, as BH_4^- is stable in base and hydrolyzes to H_2 in acid,[20,21] while CAN is most soluble in nitric acid and precipitates as $Ce(OH)_4$[22] in base. Both fuel and oxidant begin their reactions at the practical limits of an aqueous system, with current onsets immediately positive of H_2 production and negative of O_2 production, respectively, at Pt, for a practical maximum open-circuit voltage (OCV) of ∼2.3 V for a pH 0 and pH 14 system.[11,12] Our system nearly realized this full potential, with observed OCV values varying between 2 and 2.2 V. The fast kinetic processes translated a 0.5 V sacrifice in voltage to a gain in power of 75 mW/cm² (Figure 1).

Though the selected fuel (BH_4^-) and oxidant (CAN) showed exceptional performance, several limitations in power density were noted. The hydrolysis of BH_4^- in bulk solution is first-order with respect to $[BH_4^-]$,[20] so $[BH_4^-]$ was limited to 0.15 M to prevent H_2 bubble formation, which would have disrupted both uniaxial and chaotically mixed flows in the fuel cell. Plots of electrode potential vs cell voltage (Figure 2) indicated that BH_4^- limited the power output at higher voltages, so overall, the restriction on $[BH_4^-]$ prevented higher power densities from being realized. We found that 0.5 M CAN in 1 M HNO_3 matched the fuel performance under these conditions. If higher $[BH_4^-]$ can be effected, CAN will eventually become limiting, as we found it to be soluble only to ∼2.5 M. These relatively low concentrations of fuel and oxidant translate to low volumetric energy density for the system as a whole.

Employing a microfluidic, laminar-flow system provides the exceptional advantage of fuel cell operation without a selectively permeable membrane,[23] as demonstrated by our group and other workers.[8,13] However, the uniaxial flow that

dx.doi.org/10.1021/ja211751k | J. Am. Chem. Soc. 2012, 134, 6076−6079

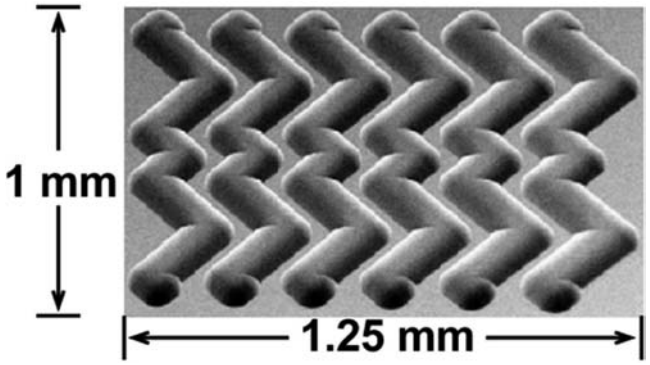

Figure 3. SEM image of staggered herringbone grooves in glass, which induce chaotic flow to separately mix the fuel and oxidant solutions. Groove depth is 50 μm.

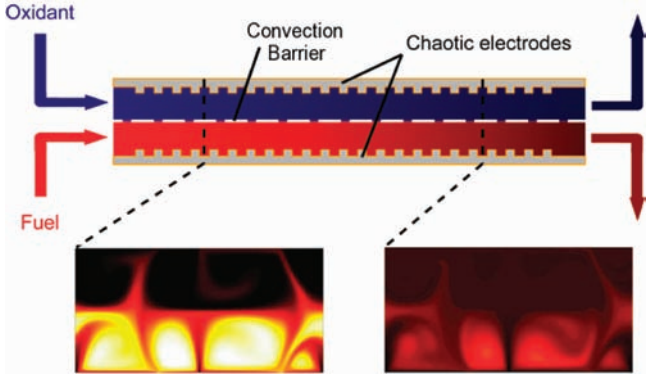

Figure 4. Simulated visualization of the approximate cross-sectional chaotic flow produced by grooved electrodes. The flow creates separate convection cells in the fuel and oxidant streams that are stirred symmetrically. There is neither convective transport through the interface between streams nor significant mixing of the streams.

aids in separation of fuel and oxidant streams also keeps unused layers of fuel and oxidant from reaching the anode and cathode, respectively, resulting in the lower current densities shown by the dotted lines in Figure 1, as well as low fuel conversion efficiencies. To overcome this challenge, a staggered-herringbone pattern of grooves was etched into the substrate of the anode and cathode before metallization (see the Supporting Information for details of the fuel cell components, geometry, and electrode fabrication). A scanning electron microscopy (SEM) image of a half-cycle of the grooves is shown in Figure 3. The grooves on the anode and cathode are aligned symmetrically, such that the normal components of the flow on opposite sides of the barrier are equal and opposite. This patterning creates separate, balanced, chaotically mixed regions in the fuel and oxidant streams, bringing unreacted fuel and oxidant to their respective electrodes. The symmetric stirring and the convection barrier prevent the two streams from mixing with one another,[10] as shown in Figure 4. The staggered-herringbone pattern is repeated four times across the 1 mm width of each channel (Figure 3), and results in four convection cells in each stream of chaotic flow (Figure 4). Maximum current density more than tripled, and maximum power doubled (Figure 1).

Current density also increased with increasing flow rate (Q, mL/min) and was found to be roughly proportional to $Q^{2/3}$. This result demonstrates scaling faster than that expected at a flat, stationary surface ($Q^{1/3}$), and faster even than that expected at a slipping surface ($Q^{1/2}$).[10] Further investigation is needed to determine the mechanism responsible for the rapid scaling of the current density with flow rate.

Our system represents a significant step forward in the development and understanding of fundamental electrochemistry and fluid mechanics essential to the establishment of low-cost, high-power-density fuel cells. By eliminating the PEM, replacing O_2 with a higher-power oxidant, preventing poisoning from CO at the anode and poisoning from MeOH crossover at the cathode, and enhancing mass transport to the electrodes, the fuel cell presented here overcomes many of the existing challenges to fuel cell technology. Overall power densities, efficiencies, and volumetric energy densities must still be addressed, and will likely require enhancing the stability of BH_4^- at high concentrations, finding a more soluble oxidant than CAN, and developing superior microfluidic transport.

■ ASSOCIATED CONTENT

Supporting Information

Experimental section. This material is available free of charge via the Internet at http://pubs.acs.org.

■ AUTHOR INFORMATION

Corresponding Author

hda1@cornell.edu

Author Contributions

[§]These authors contributed equally.

Notes

The authors declare no competing financial interest.

■ ACKNOWLEDGMENTS

The authors gratefully acknowledge support from the Office of Basic Energy Sciences, Division of Materials Sciences, U.S. Department of Energy, under Grant DE-FG02-05ER46250.

■ REFERENCES

(1) Kakaç, S.; Pramuanjaroenkij, A.; Vasiliev, L. *Mini-Micro Fuel Cells: Fundamentals and Applications*; Springer: Dordrecht, The Netherlands, 2008.

(2) Molburg, J. C.; Doctor, R. D. 20th Annual International Pittsburgh Coal Conference, Pittsburgh, PA, 2003.

(3) Kordesch, K.; Simader, G. *Fuel Cells and Their Applications*; Wiley-VCH: Weinheim, Germany, 1996.

(4) Dillon, R.; Srinivasan, S.; Aricò, A. S.; Antonucci, V. *J. Power Sources* **2004**, *127*, 112.

(5) Ma, J.; Choudhury, N. A.; Sahai, Y. *Renewable Sustainable Energy Rev.* **2010**, *14*, 183.

(6) Jayashree, R. S.; Egas, D.; Spendelow, J. S.; Natarajan, D.; Markoski, L. J.; Kenis, P. J. A. *Electrochem. Solid-State Lett.* **2006**, *9*, A252.

(7) TIAX LLC. *Cost Analysis of Fuel Cell Systems for Transportation*; Report DE-SCO2-98EE50526, October 2004.

(8) Cohen, J. L.; Westly, D. A.; Pechenik, A.; Abruña, H. D. *J. Power Sources* **2005**, *139*, 96.

(9) Cohen, J. L.; Volpe, D. J.; Westly, D. A.; Pechenik, A.; Abruña, H. D. *Langmuir* **2005**, *21*, 3544.

(10) Kirtland, J. D.; Siegel, C. R.; Stroock, A. D. *New J. Phys.* **2009**, *11*, No. 075028.

(11) Finkelstein, D. A.; Mota, N. D.; Cohen, J. L.; Abruña, H. D. *J. Phys. Chem. C* **2009**, *113*, 19700.

(12) Finkelstein, D. A.; Kirtland, J. D.; Mota, N. D.; Stroock, A. D.; Abruña, H. D. *J. Phys. Chem. C* **2011**, *115*, 6073.

(13) Kjeang, E.; Djilali, N.; Sinton, D. *J. Power Sources* **2009**, *186*, 353.

(14) Winter, M.; Brodd, R. J. *Chem. Rev.* **2004**, *104*, 4245.
(15) Taylor, A. D.; Lucas, B. D.; Guo, L. J.; Thompson, L. T. *J. Power Sources* **2007**, *171*, 218.
(16) Kjeang, E.; Michel, R.; Harrington, D. A.; Djilali, N.; Sinton, D. *J. Am. Chem. Soc.* **2008**, *130*, 4000.
(17) Kjeang, E.; Proctor, B. T.; Brolo, A. G.; Harrington, D. A.; Djilali, N.; Sinton, D. *Electrochim. Acta* **2007**, *52*, 4942.
(18) ΔG (J/mol) is the Gibbs free energy of the reaction; F (C) is Faraday's constant; $V_{\Delta pH}$ (V) is the voltage increase from a pH gradient with fuel in base and oxidant in acid; R (J K^{-1} mol^{-1}) is the universal gas constant; T (K) is the absolute temperature; and K_w is the dissociation constant for H_2O.
(19) $V_{\Delta pH}$ can also be determined using the expected increase in E (electrochemical potential, V) of 0.059 V for each unit decrease in pH. Thus an oxidant in solution of pH 0 vs pH 14 has an increased potential of 0.826 V, and adds 0.826 V to the voltage of a reaction with a fuel at pH 14.
(20) Morris, J. H.; Gysling, H. J.; Reed, D. *Chem. Rev.* **1985**, *85*, 51.
(21) Pecsok, R. L. *J. Am. Chem. Soc.* **1953**, *75*, 2862.
(22) Sherrill, M. S.; King, C. B.; Spooner, R. C. *J. Am. Chem. Soc.* **1943**, *65*, 170.
(23) Morse, J. D. *Int. J. Energy Res.* **2007**, *31*, 576.